

# Laboratory Study on the Hygroscopic Behavior of External and Internal C<sub>2</sub>–C<sub>4</sub> Dicarboxylic Acid–NaCl Mixtures

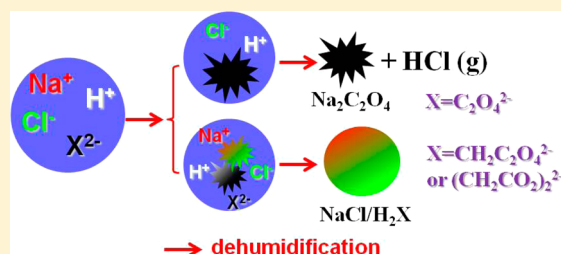
Qingxin Ma,<sup>†</sup> Jinzhu Ma,<sup>†</sup> Chang Liu,<sup>‡</sup> Chengyue Lai,<sup>†</sup> and Hong He<sup>†,\*</sup>

<sup>†</sup>Research Center for Eco-Environmental Sciences, Chinese Academy of Sciences, Beijing, China

<sup>‡</sup>Chinese Academy of Meteorological Sciences, Beijing, China

## Supporting Information

**ABSTRACT:** Atmospheric aerosol is usually found to be a mixture of various inorganic and organic components in field measurements, whereas the effect of this mixing state on the hygroscopicity of aerosol particles has remained unknown. In this study, the hygroscopic behavior of mixtures of C<sub>2</sub>–C<sub>4</sub> dicarboxylic acids and NaCl was investigated. For both externally and internally mixed malonic acid–NaCl and succinic acid–NaCl particles, correlation between water content and chemical composition was observed and the water content of these mixtures at relative humidity (RH) above 80% can be well predicted by the Zdanovskii–Stokes–Robinson (ZSR) method. In contrast, a nonlinear relation between the total water content of the mixtures and the water content of each chemical composition separately was found for oxalic acid–NaCl mixtures. Compared to the values predicted by the ZSR method, the dissolution of oxalic acid in external mixtures resulted in an increase in the total water content, whereas the formation of less hygroscopic disodium oxalate in internal mixtures led to a significant decrease in the total water content. Furthermore, we found that the hygroscopicity of the sodium dicarboxylate plays a critical role in determining the aqueous chemistry of dicarboxylic acid–NaCl mixtures during the humidifying and dehumidifying process. It was also found that the hydration of oxalic acid and the deliquescence of NaCl did not change in external oxalic acid–NaCl mixtures. The deliquescence relative humidity (DRHs) for both malonic acid and NaCl decreased in both external and internal mixtures. These results could help in understanding the conversion processes of dicarboxylic acids to dicarboxylate salts, as well as the substitution of Cl by oxalate in the atmosphere. It was demonstrated that the effect of coexisting components on the hygroscopic behavior of mixed aerosols should not be neglected.



## 1. INTRODUCTION

Hygroscopicity is one of the most important properties of atmospheric aerosol particles. Hygroscopic salts in atmospheric aerosols can take up water from the ambient atmosphere, which then induces the growth of particles and converts solid particles to aqueous droplets after deliquescence.<sup>1</sup> The change in size and phase of aerosol particles further influences their light scattering, atmospheric lifetime and chemical reactivity.<sup>2</sup> The hygroscopic properties of aerosol also determine which fraction of aerosol particles can act as cloud condensation nuclei (CCNs) and thus contribute to the aerosol indirect effect.<sup>3</sup> Due to its great importance, the hygroscopic behavior of aerosol particles as well as the related atmospheric processes has been a major focus of atmospheric sciences.

Sea salt aerosol is one of the major sources of naturally produced airborne particles and plays an important role in tropospheric chemistry and the atmospheric environment.<sup>4–6</sup> (and references therein) As a main component of sea salt aerosol, NaCl is considered a representative hygroscopic salt, and the hygroscopic behavior of pure NaCl has been investigated thoroughly.<sup>1,7–18</sup> In addition, NaCl mixed with inorganic and organic species has been frequently detected in field measurements in marine atmospheres.<sup>19–25</sup> Therefore, the

effect of coexisting components on the hygroscopic behavior of NaCl has also received much attention. For instance, the water activity of mixtures of NaCl with MgSO<sub>4</sub>, Na<sub>2</sub>SO<sub>4</sub>, or MgCl<sub>2</sub> were studied.<sup>26</sup> Good agreement was found between the predictions of the Zdanovskii–Stokes–Robinson (ZSR) and Kusik–Meissner (KM) models and the experimental data over the entire range of water activity before the onset of crystallization for all mixtures studied.

Dicarboxylic acids (DCAs, or diacids) are ubiquitous in the atmosphere and represent a significant portion of the organic fraction of aerosols.<sup>27–35</sup> The sources of DCAs include direct emission from automobiles and biomass burning,<sup>28</sup> as well as oxidation of volatile organic compounds (VOCs) in photochemistry and in-cloud processes.<sup>31,33,36,37</sup> Due to their strong hydrophilic and hygroscopic properties, DCAs are able to reduce the surface tension of CCNs, which consequently affect cloud formation and the global radiation balance.<sup>38,39</sup> Oxalic acid (C<sub>2</sub>), malonic acid (C<sub>3</sub>), and succinic acid (C<sub>4</sub>) are

Received: May 23, 2013

Revised: July 31, 2013

Accepted: August 13, 2013

Published: August 13, 2013

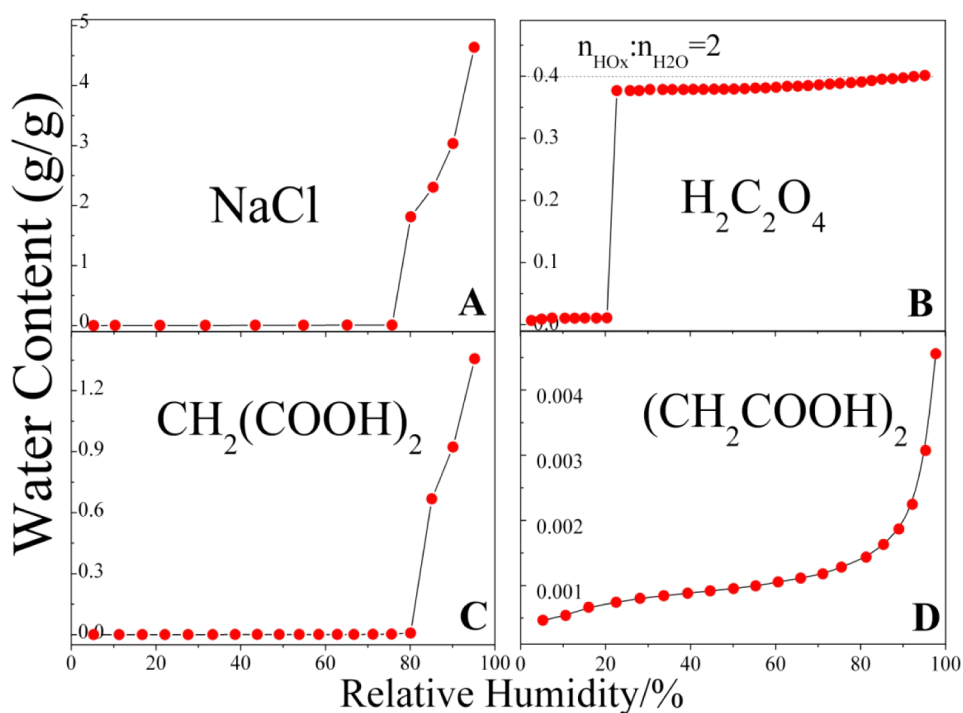


**Figure 1.** Water adsorption isotherms of (A) sodium chloride ( $m = 8.8$  mg), (B) oxalic acid ( $m = 90.0$  mg), (C) malonic acid ( $m = 11.2$  mg), and (D) succinic acid ( $m = 86.5$  mg) at  $5$  °C.

usually the most abundant DCAs in atmospheric aerosols, and have been frequently detected mixed with sea salt particles.<sup>19,22,31,40</sup> The hygroscopic properties of these three DCAs have been studied widely.<sup>41–44</sup> On the other hand, chloride depletion in sea-salt aerosols association with inorganic and organic anions is always found in marine atmospheres.<sup>19,24</sup> Substitution of chloride in sea-salt particles by carboxylic acids has been suggested.<sup>19,25</sup> Better understanding of the chemistry associated with sea-salt particles requires the investigation of reactions in deliquescent sea-salt particles. The deliquescence and hygroscopic growth of internally mixed NaCl–glutaric acid and NaCl–pinonic acid mixtures were measured with a hygroscopic tandem differential mobility analyzer (H-TDMA) system.<sup>45</sup> The results showed that these organic acids had no effect on the deliquescence relative humidity (DRH) of NaCl, and the hygroscopic growth factors (GFs) of the mixtures agreed with the predictions of the ZSR approach. Pope et al. also found that the properties of the aqueous mixtures of malonic acid and glutaric acid with NaCl could be estimated well based on those of the pure solutions.<sup>46</sup> Thus, all these previous studies showed a correlation between hygroscopicity and the chemical compositions of NaCl and DCAs mixtures. However, the interactions and chemical processes between NaCl and DCAs during humidifying and dehumidifying processes needs further investigation, since substitution of chloride by dicarboxylates has been detected in field measurements.

In this study, the hygroscopic behaviors of externally and internally mixed DCAs and NaCl particles were investigated. Oxalic acid, malonic acid, and succinic acid were chosen as the surrogates of DCAs. Whether a linear or nonlinear relation exists between hygroscopicity and the quantities of different chemical compositions in NaCl–DCAs mixtures was determined. The main focus of this study is the effect of mixing status on the hygroscopic behavior of particles containing

DCAs and NaCl, as well as the mechanism responsible for nonlinear behavior.

## 2. EXPERIMENTAL SECTION

**Vapor Sorption Analyzer Experiments.** Water adsorption isotherms were measured with a modified vapor sorption analyzer at  $5$  °C. The method has been described in a previous article.<sup>17</sup> (see detailed description in Supporting Information (SI)) Briefly, the vapor sorption analyzer was obtained by modifying a  $N_2$  adsorption–desorption analyzer, which is used in characterizing the surface area of solid materials. Water vapor instead of nitrogen was used as the adsorbate in studying the hygroscopicity of particles. The relative humidity (RH) was referred to the relative pressure ( $P/P_0$ ), in which  $P_0$  was set as the saturation vapor pressure at the temperature of the sample. When values of  $P_0$  and RH points were established, then the absolute pressure around the sample was controlled automatically by computer program. By adjusting the speed of the turbo pump, the pressure accuracy can be controlled at the level of  $10^{-4}$  Torr, which makes the uncertainty less than 1%. For the hygroscopic behavior study, we set the sensitivity of the instrument to yield an uncertainty of 2%, in order to shorten the experiment time. The particles were evacuated at room temperature for 1 h at a pressure of  $10^{-3}$  Torr. The evacuated particles were then exposed to vapor with different RH to determine the adsorption isotherm by calculating the pressure change during the equilibrium process.

**Raman Spectroscopy.** Raman spectroscopy has been proven to be a powerful tool and is widely used to investigate the heterogeneous reactions and hygroscopic behavior of aerosol. Raman spectra were recorded on a UV/vis resonance Raman spectrometer (UVR DLPC-DL-03), which has been described in a previous article.<sup>47</sup> In previous studies, a continuous diode-pumped solid state (DPSS) laser beam (532 nm) was used as the exciting radiation. The visible light

laser, however, induced intense fluorescence for NaCl–DCAs mixtures and showed very low signal-to-noise ratio. Therefore, in this study, a UV laser beam (He–Cd, 325 nm) was used as the exciting radiation to avoid fluorescence interference. The diameter of the laser spot on the sample surface was focused at 25  $\mu\text{m}$ . The spectral resolution was 2.0  $\text{cm}^{-1}$ . The instrument was calibrated against the Stokes Raman signal of Teflon at 1378  $\text{cm}^{-1}$ . The temperature and relative humidity in the Raman room was maintained at 25  $^{\circ}\text{C}$  and <40% RH. Sample powder was placed into an aluminum sample holder and could be purged with  $\text{N}_2$ . The laser heating effect could be neglected because the power is less than 10 mW and the Raman spectra were not changed after illumination for 1h.

**Chemicals.** NaCl (sodium chloride), NaOH (sodium hydroxide),  $\text{H}_2\text{C}_2\text{O}_4 \cdot 2\text{H}_2\text{O}$  (oxalic acid dihydrate),  $\text{CH}_2(\text{COOH})_2$  (malonic acid), and  $(\text{CH}_2\text{COOH})_2$  (succinic acid) used in this work are all of analytical reagent grade with purity greater than 99.5%. All samples were used as purchased (from Sinopharm Chemical Reagent Co. Ltd.). Sodium dicarboxylate salts were prepared from internally mixed NaOH–DCA solutions, which were used for comparison with NaCl–DCA mixtures and to determine whether chemical reactions occurred or not. The molar ratio of NaCl or NaOH with each DCA in all experiments was 2/1 according to the stoichiometry. Particle samples were prepared in the same manner for all tested mixtures. Externally mixed particles were prepared by mixing and grinding different components together. Internally mixed particles were prepared by atomizing solutions of NaCl (or NaOH) and DCA with total Na concentration of 0.1 M. Liquid particles were nebulized from solutions, and then after being dried in a diffusion dryer, particles were collected on a fiberglass filter. In this way, some submicrometer particles may not be collected. Distilled  $\text{H}_2\text{O}$  was degassed by heating prior to use.

### 3. RESULTS AND DISCUSSION

**3.1. Water Adsorption Isotherms of Individual Components.** Figure 1 shows the water adsorption isotherms of NaCl, oxalic acid, malonic acid, and succinic acid. These isotherms exhibited quite different characters. Water adsorption on NaCl was measured first, as shown in Figure 1A. The deliquescence point for NaCl was determined to be 75% RH, which is in good agreement with previous studies.<sup>9,12,13,26,45,48,49</sup> As for oxalic acid (Figure 1B), the water content showed an abrupt increase at 20% RH and then increased slightly as RH increased. This phenomenon was due to the conversion of anhydrous oxalic acid ( $\text{H}_2\text{C}_2\text{O}_4$ ) to dihydrate particles ( $\text{H}_2\text{C}_2\text{O}_4 \cdot 2\text{H}_2\text{O}$ ), as discussed in previous studies.<sup>50,51</sup> No deliquescence of oxalic acid was observed even when RH was increased to 95% RH. This result was in agreement with Peng et al.<sup>41</sup> and Braban et al.<sup>43</sup> As for malonic acid (Figure 1C), the water content was very small at low RH. When RH was increased to 80% RH, the water content exhibited an abrupt growth and then increased quickly with increasing RH, indicating the deliquescence of malonic acid. Although Peng et al.<sup>41</sup> reported that no deliquescence of malonic acid in the RH range of 5–93% was observed in the electronic dynamic-balance (EDB) study, DRHs of malonic acid were determined to be about 79% RH at 5  $^{\circ}\text{C}$ <sup>43</sup> and about 80.6% at 4  $^{\circ}\text{C}$ .<sup>52</sup> Thus, the DRH for malonic acid was determined to be 80% RH in this study. As for succinic acid (Figure 1D), the water adsorption isotherm exhibits a multilayer adsorption characteristic. This suggests that water

was only adsorbed on the surface of succinic acid particles, and no phase transformation occurred during the adsorption process. The hygroscopic behavior of succinic acid has been studied widely.<sup>41,42,44,52,53</sup> No deliquescence was observed and the growth factor was determined to be 1.0 in the RH range of 0–95%, which was consistent with the results in the present study.

The isotherms of pure particles were used to calculate the theoretical water content of mixed particles according to the ZSR method.<sup>26,54</sup> This approach assumes that the water content of a mixed particle is equal to the sum of the liquid water contents of the individual pure components at the same relative humidity.<sup>45,55,56</sup> The ZSR equation can be written using water contents as

$$m = \sum a_i \cdot m_i \quad (1)$$

where  $m$  is the water content of the mixture,  $a_i$  and  $m_i$  are the mass fraction of each component in dry mixtures and the water content of species  $i$ , respectively. Water content was recorded as mass of water adsorption/absorption per gram of sample, that is, g (water)/g (sample).

**3.2. Water Adsorption Isotherms of NaCl–DCAs Mixtures.**  $\text{H}_2\text{C}_2\text{O}_4$  Mixtures. Figure 2 shows the water

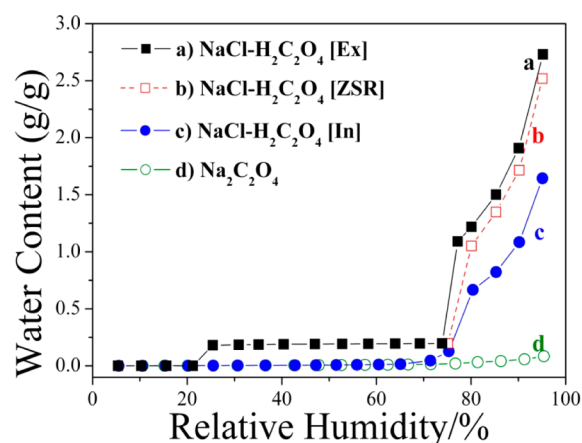


**Figure 2.** Water adsorption isotherms of (a) NaCl– $\text{H}_2\text{C}_2\text{O}_4$  external mixture (black line,  $m = 10.6$  mg), (b) the ZSR predicted curve of NaCl– $\text{H}_2\text{C}_2\text{O}_4$  mixture (red line), (c) NaCl– $\text{H}_2\text{C}_2\text{O}_4$  internal mixture (blue line,  $m = 11.4$  mg), and (d)  $\text{Na}_2\text{C}_2\text{O}_4$  (green line,  $m = 96.5$  mg).

isotherms of NaCl– $\text{H}_2\text{C}_2\text{O}_4$  mixtures in different mixing states, as well as that of  $\text{Na}_2\text{C}_2\text{O}_4$  particles. Water contents of NaCl– $\text{H}_2\text{C}_2\text{O}_4$  mixtures above 75% RH predicted by the ZSR approach are also shown in Figure 2. In the figures below, [Ex], [In], and [ZSR] represent external mixture, internal mixture, and the ZSR prediction, respectively. For externally mixed NaCl– $\text{H}_2\text{C}_2\text{O}_4$  particles (line a), the transformation of anhydrous oxalic acid to dihydrate particles occurred at 20% RH, which was close to the transition point of pure oxalic acid. This implied that the externally mixed NaCl does not affect the transformation of  $\text{H}_2\text{C}_2\text{O}_4$ . The measured DRH of externally mixed NaCl– $\text{H}_2\text{C}_2\text{O}_4$  particles was 75% RH, the same as that of pure NaCl, suggesting that the externally mixed  $\text{H}_2\text{C}_2\text{O}_4$  has no effect on the deliquescence of NaCl. When the RH was above 75% RH, however, water contents of externally mixed NaCl– $\text{H}_2\text{C}_2\text{O}_4$  particles were higher than those predicted from the ZSR approach (line b). This is due to the dissolution of  $\text{H}_2\text{C}_2\text{O}_4$  in deliquescent NaCl solution, which led to the

decrease in the surface tension of NaCl solution and subsequent increase of the water absorption capacity. As for internally mixed NaCl–H<sub>2</sub>C<sub>2</sub>O<sub>4</sub> particles (line c), the hygroscopic behavior is quite different from that of externally mixed particles. No transition point for hydrated oxalic acid and no obvious deliquescence point were observed. The water content above 80% RH of internally mixed NaCl–H<sub>2</sub>C<sub>2</sub>O<sub>4</sub> particles was much lower than those of externally mixed NaCl–H<sub>2</sub>C<sub>2</sub>O<sub>4</sub> particles (line a) and the ZSR predicted values (line b). For example, the water content of internally mixed NaCl–H<sub>2</sub>C<sub>2</sub>O<sub>4</sub> particles was 0.82 g/g at 85% RH, much smaller than the value of externally mixed particles (1.50 g/g) and the ZSR calculated value (1.34 g/g). The decrease in the water content may be due to reaction between NaCl and H<sub>2</sub>C<sub>2</sub>O<sub>4</sub> during the drying process of the internal mixture, producing less hygroscopic components in the mixture. We further measured the water adsorption isotherm of Na<sub>2</sub>C<sub>2</sub>O<sub>4</sub> particles. As seen in Figure 2 (line d), Na<sub>2</sub>C<sub>2</sub>O<sub>4</sub> shows less hygroscopicity, with no deliquescence and no quick increase in water content at high RH. By studying the water cycle of Na<sub>2</sub>C<sub>2</sub>O<sub>4</sub> with EDB, Peng and Chan found that as RH increased to 93%, deliquescence was not observed and the total mass fraction of solute (*mfs*) was not changed.<sup>57</sup> Another study by H-TDMA also reported that the growth factor for Na<sub>2</sub>C<sub>2</sub>O<sub>4</sub> remained 1.0 below 90% RH.<sup>58</sup> Therefore, Na<sub>2</sub>C<sub>2</sub>O<sub>4</sub> may be formed in the internally mixed NaCl–H<sub>2</sub>C<sub>2</sub>O<sub>4</sub> particles, causing the decrease in water content. According to eq 1, the mass fraction of Na<sub>2</sub>C<sub>2</sub>O<sub>4</sub> in the internal mixtures was calculated to be about 60–80%. The water content for externally mixed NaCl–H<sub>2</sub>C<sub>2</sub>O<sub>4</sub> particles did not decrease during the humidifying process, implying that no reaction occurred in the humidifying process. Thus, the formation of Na<sub>2</sub>C<sub>2</sub>O<sub>4</sub> may occur in the dehumidifying process of NaCl–H<sub>2</sub>C<sub>2</sub>O<sub>4</sub> mixture droplets.

**CH<sub>2</sub>(COOH)<sub>2</sub> Mixtures.** Figure 3 shows the water adsorption isotherms of NaCl–CH<sub>2</sub>(COOH)<sub>2</sub> mixtures with different

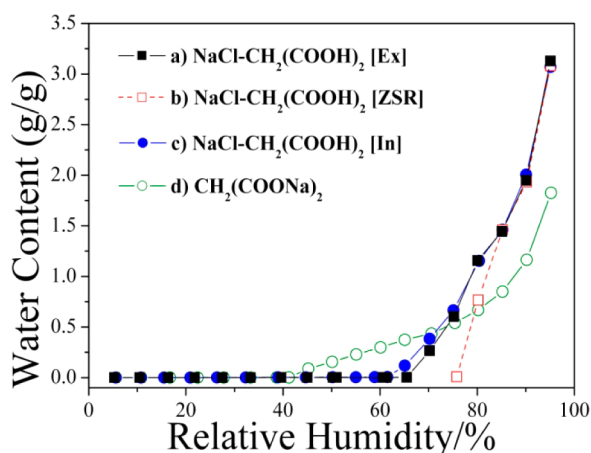


**Figure 3.** Water adsorption isotherms of (a) NaCl–CH<sub>2</sub>(COOH)<sub>2</sub> external mixture (black line, *m* = 9.6 mg), (b) the ZSR predicted curve of NaCl–CH<sub>2</sub>(COOH)<sub>2</sub> mixture (red line), (c) NaCl–CH<sub>2</sub>(COOH)<sub>2</sub> internal mixture (blue line, *m* = 11.4 mg), and (d) CH<sub>2</sub>(COONa)<sub>2</sub> (green line, *m* = 9.3 mg).

mixing states, as well as that of CH<sub>2</sub>(COONa)<sub>2</sub> particles. Externally (line a) and internally (line c) mixed NaCl–CH<sub>2</sub>(COOH)<sub>2</sub> particles exhibited DRH in the range of 65–70% RH and 60–65% RH, respectively, which are lower than the DRHs for NaCl (75% RH) and CH<sub>2</sub>(COOH)<sub>2</sub> (80% RH).

This is in good agreement with the work of Pope et al.,<sup>46</sup> in which the DRH for NaCl–CH<sub>2</sub>(COOH)<sub>2</sub> mixtures was observed to be 67% RH. This implied that the deliquescence of NaCl and CH<sub>2</sub>(COOH)<sub>2</sub> could be affected by the mixing process. However, the water contents for both internally and externally mixed NaCl–CH<sub>2</sub>(COOH)<sub>2</sub> particles were close to those of the ZSR predicted values (line b) at high RH. If the water content of particles depends on their components, this result indicates that the chemical compositions of mixed NaCl–CH<sub>2</sub>(COOH)<sub>2</sub> particles were not changed after mixing. Pope et al. also found that water and solute activities in NaCl–CH<sub>2</sub>(COOH)<sub>2</sub> aqueous particles could be fitted by the ZSR approach.<sup>46</sup> The values measured for mixed particles were larger than the ZSR-predicted value when RH was below 85% RH. This is because the dissolution of coexisting compounds can reduce the surface tension of solutions and enhance water absorption. Disodium malonate, CH<sub>2</sub>(COONa)<sub>2</sub>, took up water continuously above 40% RH (line d), although this point could not be defined as the DRH of CH<sub>2</sub>(COONa)<sub>2</sub>. Previous studies also reported that disodium malonate particles continued to grow with increasing RH, and no deliquescence point was observed.<sup>57,58</sup> All these studies demonstrated that CH<sub>2</sub>(COONa)<sub>2</sub> particles are hygroscopic.

**(CH<sub>2</sub>COOH)<sub>2</sub> Mixtures.** Figure 4 shows the water adsorption isotherms of NaCl–(CH<sub>2</sub>COOH)<sub>2</sub> mixtures with different

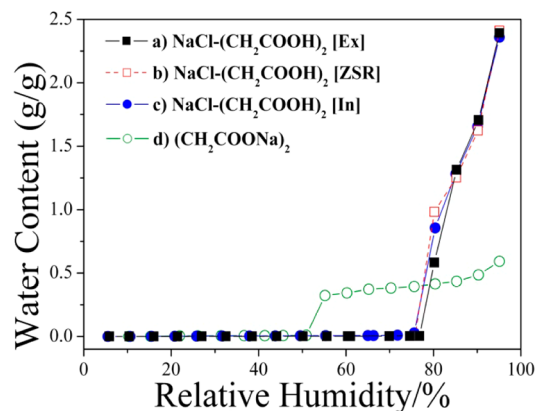


**Figure 4.** Water adsorption isotherms of (a) NaCl–(CH<sub>2</sub>COOH)<sub>2</sub> external mixture (black line, *m* = 12.3 mg), (b) the ZSR predicted curve of NaCl–(CH<sub>2</sub>COOH)<sub>2</sub> mixture (red line), (c) NaCl–(CH<sub>2</sub>COOH)<sub>2</sub> internal mixture (blue line, *m* = 15.6 mg), and (d) CH<sub>2</sub>(COONa)<sub>2</sub> (green line, *m* = 9.7 mg).

mixing states. It is interesting to note that the hygroscopic behavior of both externally (line a) and internally (line c) mixed NaCl–(CH<sub>2</sub>COOH)<sub>2</sub> particles was quite similar to that of the ZSR calculated curve when RH was above 85% (line b). The values measured for mixed particles were smaller than the ZSR-predicted value at 80% RH. This is due to the blocking effect of coexisting (CH<sub>2</sub>COOH)<sub>2</sub> on the water adsorption on NaCl, since (CH<sub>2</sub>COOH)<sub>2</sub> is not hygroscopic. This indicated that mixing NaCl and (CH<sub>2</sub>COOH)<sub>2</sub> particles can affect the hygroscopic behavior of both compounds at low RH. However, no decrease in water content at high RH occurred for mixed NaCl–(CH<sub>2</sub>COOH)<sub>2</sub> particles indicating chemical compositions were not changed, which was also confirmed by Raman characterization results (seen in Figure S2 in the SI). Sodium succinate, prepared from NaOH–(CH<sub>2</sub>COOH)<sub>2</sub> internal mixtures, shows the DRH at 50% RH (line d). Peng and Chan reported that the DRH of sodium succinate appears at

63.5–66% RH.<sup>57</sup> Wu et al. observed continuous growth of sodium succinate with no deliquescence point, and they explained this result as arising from the effect of temperature on solubility or from impurities in solution.<sup>58</sup> These results demonstrate that sodium succinate is hygroscopic and readily takes up water from the ambient atmosphere.

**3.3. Raman Spectra of NaCl–DCAs Mixtures.**  $H_2C_2O_4$  Mixtures. To confirm the species in each mixture, we used Raman spectra to analyze the chemical compositions. As shown in Figure 5, externally mixed NaCl– $H_2C_2O_4$  (line b) particles

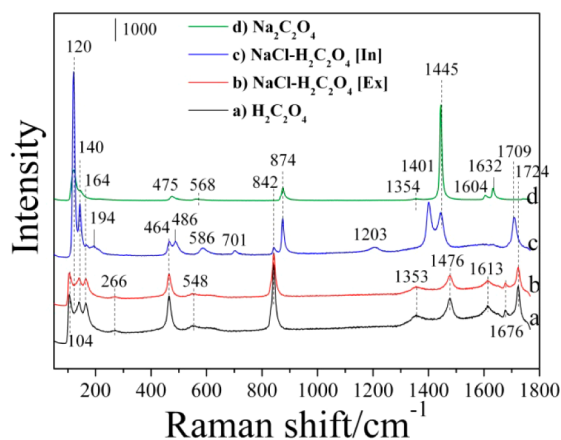


**Figure 5.** Raman spectra of (a)  $H_2C_2O_4$  (black line), (b) NaCl– $H_2C_2O_4$  external mixture (red line), (c) NaCl– $H_2C_2O_4$  internal mixture (blue line), and (d)  $Na_2C_2O_4$  (green line).

give a spectrum similar to that of pure  $H_2C_2O_4$  (line a) because NaCl has no Raman shift peaks.<sup>51</sup> The decrease in intensity was due to the dilution effect of the coexisting NaCl. According to the assignments of oxalic acid in the literature, the peaks at 1724, 1353, 842, and 464  $cm^{-1}$  can be assigned to the stretching mode of C=O, C–OH, C–C, and the out of plane bending mode of C=O, respectively.<sup>59–61</sup> The peak at 1676  $cm^{-1}$  is due to the coupled C=O and C–O stretching modes.<sup>61</sup> The peak at 1476  $cm^{-1}$  is due to the COH deformation coupled to C–O and C–C stretching.<sup>61</sup> The peak at 548  $cm^{-1}$  is attributed to the in-plane deformation of COOH.<sup>61</sup> The peaks at 164, 140, and 104  $cm^{-1}$  have been attributed to the translational lattice vibration of water molecules.<sup>59,60</sup> In the spectrum of internally mixed NaCl– $H_2C_2O_4$  particles (line c), the intensity of peaks at 104, 266, 464, 548, 842, 1353, 1476, 1613, 1676, and 1724  $cm^{-1}$  attributed to  $H_2C_2O_4$  decreased greatly, indicating the depletion of  $H_2C_2O_4$  due to the reaction between NaCl and  $H_2C_2O_4$  in the atomizing and drying process. Several new peaks at 120, 194, 486, 586, 701, 874, 1203, 1401, 1445, and 1709  $cm^{-1}$  were observed in the spectrum of internally mixed NaCl– $H_2C_2O_4$  particles (line c), while peaks at 120, 874, and 1445  $cm^{-1}$  were also observed in the spectrum of  $Na_2C_2O_4$  particles (line d). In addition, several peaks at 475, 568, 1354, 1604, and 1632  $cm^{-1}$  were observed in the spectrum of  $Na_2C_2O_4$  particles. All these peaks can be found in the spectra of natural  $Na_2C_2O_4$  particles.<sup>62</sup> The peaks at 1632 and 1604  $cm^{-1}$  were assigned to the asymmetric C=O stretching mode, while those at 1445 and 1354  $cm^{-1}$  were assigned to the  $\nu(C-O)$  stretching mode and the OCO wag mode, respectively. The band at 874  $cm^{-1}$  was assigned to the  $\nu(C-C)$  stretching mode.<sup>62</sup> These results suggest that  $Na_2C_2O_4$  was formed in the internal NaCl– $H_2C_2O_4$  mixtures, which is in agreement with the vapor

sorption results and was also confirmed by ATR-FTIR characterization results (seen in Figure S3 in the SI).

$CH_2(COOH)_2$  Mixtures. In the case of  $CH_2(COOH)_2$  mixtures, both externally mixed (line b) and internally mixed (line c) NaCl– $CH_2(COOH)_2$  particles showed Raman spectra similar to that of pure  $CH_2(COOH)_2$  particles (line a), as seen in Figure 6. There was no new peak or peak shift observed in

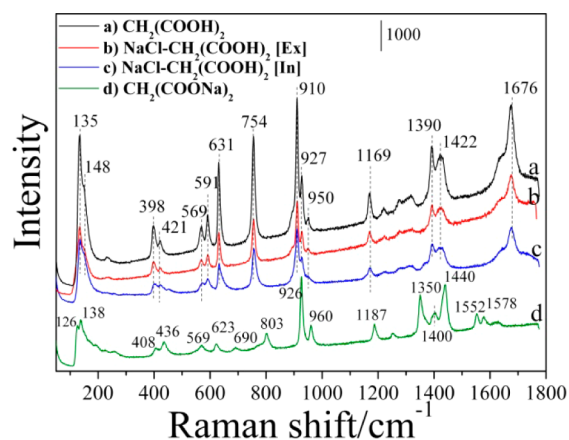


**Figure 6.** Raman spectra of (a)  $CH_2(COOH)_2$  (black line), (b) NaCl– $CH_2(COOH)_2$  external mixture (red line), (c) NaCl– $CH_2(COOH)_2$  internal mixture (blue line), and (d)  $CH_2(COONa)_2$  (green line).

the spectra of either externally mixed or internally mixed NaCl– $CH_2(COOH)_2$  particles compared to that of  $CH_2(COOH)_2$  particles. The decrease in peak intensity of external and internal mixtures was due to the dilution effect of coexisting NaCl. However, the Raman spectrum of  $CH_2(COONa)_2$  (line d) was very different from the spectra of  $CH_2(COOH)_2$  and NaCl– $CH_2(COOH)_2$  mixtures. These results clearly demonstrate that conversion of malonic acid and sodium chloride to disodium malonate was not observed, which was also confirmed by ATR-FTIR characterization results (seen in Figure S4 in the SI). However, in a previous study, based on the quantitative assessment of Energy Dispersive X-ray (EDX) spectra and the E-AIM model calculation, Laskin et al. suggested that reaction between malonic acid and sodium chloride took place during the mixing process.<sup>25</sup> This discrepancy may be due to the difference in the size of analyzed particles. In Laskin et al.,<sup>25</sup> submicrometer particles were analyzed by SEM. In the present study, we used a filter to collect samples; thus, some submicrometer particles, which could contain many reacted particles, may not be collected. Another probable cause is that the samples prepared in this study underwent a speedy drying process, which minimized the volatilization of HCl for NaCl–malonic acid mixture droplets. In the present work, we combined Raman spectroscopy and ATR–FTIR spectroscopy to characterize the chemical compositions in the NaCl– $CH_2(COOH)_2$  mixtures. Both results confirmed that there were no new compounds formed in the NaCl– $CH_2(COOH)_2$  mixtures after the dehumidifying process. Moreover, the water adsorption experiment results showed that the water absorption capacity of the NaCl– $CH_2(COOH)_2$  mixtures does not change, both for external and internal mixtures. Therefore, NaCl reacts with  $CH_2(COOH)_2$  during the humidifying and dehumidifying process was not observed in this study.

**3.5. Comparison of Hygroscopicity of DCAs and Sodium Salts.** The log ionization constants  $pK_1$  of oxalic acid, malonic acid, and succinic acid are 1.27, 2.83, and 4.2, respectively, which are all much greater than that of hydrogen chloride,  $-7.0$ .<sup>63</sup> Therefore, substitution of chloride by dicarboxylates is not thermodynamically favored in bulk solutions. However, in a previous study, we found that substitution of nitrate by oxalate occurred in the humidifying process of  $H_2C_2O_4-Ca(NO_3)_2$  mixtures, which was mainly due to the very low hygroscopicity and solubility of the formed  $CaC_2O_4$ .<sup>51</sup> To further analyze the difference in reactivity of different DCAs toward NaCl, we used water content at 90% RH to compare the hygroscopicity of particles.<sup>64</sup>

Water contents at 90% RH of DCAs and sodium salts are shown in Figure 7. The water content of NaCl was 3.03 g/g,

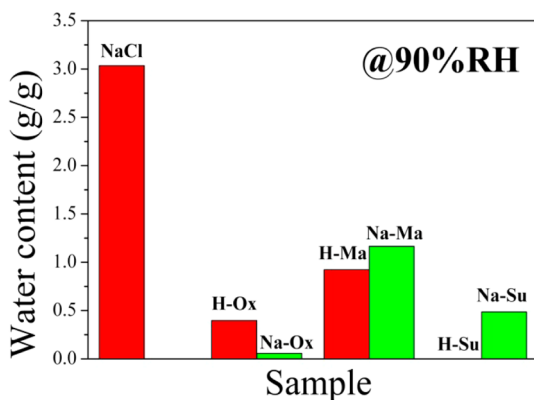


**Figure 7.** Comparison of water contents at 90% RH of DCAs and sodium salts. H-Ox: oxalic acid,  $H_2C_2O_4$ ; Na-Ox: sodium oxalate,  $Na_2C_2O_4$ ; H-Ma: malonic acid,  $CH_2(COOH)_2$ ; Na-Ma: sodium malonate,  $CH_2(COONa)_2$ ; H-Su: succinic acid,  $(CH_2COOH)_2$ ; Na-Su: sodium succinate,  $(CH_2COONa)_2$ .

the largest among all these samples. The water content of  $H_2C_2O_4$  was 0.40 g/g, which was close to the mass fraction of hydrated water in oxalic acid dihydrate. When converted to disodium oxalate, the water content decreased to less than 0.058 g/g. The GFs for oxalic acid<sup>42</sup> and disodium oxalate<sup>58</sup> determined by H-TDMA at 90% RH were 1.43 and 1.0, respectively, indicating that conversion of oxalic acid to disodium oxalate led to the reduction of hygroscopicity. Thus, during the dehumidifying process of mixed NaCl– $H_2C_2O_4$  droplets in the preparation process of internal mixture particles, nonhygroscopic disodium oxalate could form and subsequently reduce the hygroscopicity of the mixtures. The loss of water could further promote the volatilization of HCl from the droplets. Therefore, the aqueous chemistry of NaCl– $H_2C_2O_4$  droplets can involve reaction between NaCl and  $H_2C_2O_4$ .

For malonic acid and disodium malonate, the water contents were 0.92 g/g and 1.16 g/g, respectively, implying disodium malonate is slightly more hygroscopic than malonic acid. The GFs of malonic acid and disodium malonate determined by H-TDMA at 90% RH were 1.48 and 1.78, respectively, also indicating malonic acid is less hygroscopic than disodium malonate.<sup>58</sup> The results in this study are in good agreement with previous H-TDMA results. Thus, during the dehumidifying process of mixed NaCl– $CH_2(COOH)_2$  droplets, if disodium malonate is formed in the solution, it may not reduce the hygroscopicity of the mixtures and may hold

residual water, which limits the volatilization of HCl, especially when the droplets undergo a quick drying process. Therefore, the aqueous chemistry of NaCl– $CH_2(COOH)_2$  droplets may favor the formation of NaCl and  $CH_2(COOH)_2$  with no reaction taking place during the drying process, as confirmed by Raman and ATR–FTIR studies.

A clearer situation was seen in the case of succinic acid and disodium succinate, for which the water contents were 0.0018 g/g and 0.48 g/g, respectively. The GFs of succinic acid and disodium succinate determined by H-TDMA at 90% RH were 1.0 and 1.69, respectively, indicating succinic acid is much less hygroscopic than disodium succinate.<sup>58</sup> Similar to malonic acid, if disodium succinate formed in the droplets during the drying process, it could hold more water and limit HCl volatilization. Therefore, conversion of succinic acid to disodium succinate hardly occurs during the humidifying and dehumidifying process of NaCl– $(CH_2COOH)_2$  mixtures. In field measurements, Kermine et al. found that the main constituents replacing chloride from supermicrometer sea-salt particles were sulfate and nitrate followed by methanesulfonate and oxalate, while malonate and succinate gave a minor contribution.<sup>19</sup> This phenomenon is not unexpected. First, the mass fraction of oxalic acid is larger than those of malonic acid and succinic acid. Second, as shown in this study, substitution of Cl by malonate and succinate does not occur in the humidifying and dehumidifying process of NaCl–malonic acid mixtures and NaCl–succinic acid mixtures, which limits the contribution of malonate and succinate to the replacement of chloride.

#### 4. ATMOSPHERIC IMPLICATIONS

In the atmosphere, aerosol particles always contain more than one compound. It is common that several compositions coexist due to external or internal mixing. The mixing state of aerosol particles always affects their atmospheric lifetime and physicochemical properties, especially hygroscopic behavior.<sup>65</sup> It was found that oxalic and malonic acids were found to be predominantly internally mixed with mineral dust and aged sea salt particles.<sup>31</sup> In the present study, we found that the effect of the mixing state of DCAs on hygroscopic behavior depended greatly on the type of acid. Conversion of oxalic acid to disodium oxalate led to a great decrease in hygroscopicity. In a previous study, we found that most atmospherically relevant oxalates are less hygroscopic under ambient conditions.<sup>50</sup> In contrast, the transformation of malonic acid to disodium malonate resulted in a slight increase in hygroscopicity. In the case of succinic acid and disodium succinate, the conversion led to a great increase in hygroscopicity. DCAs and dicarboxylates can coexist in airborne particulates depending on a few factors (such as water content, pH, and mixing status of particulates). Therefore, when hygroscopic behavior is considered in modeling simulations, distinction should be made between dicarboxylic acids and their disodium salts.

The hygroscopic behavior of aerosols is considered to be a water adsorption/absorption–desorption cycle. Changes of particle size, water content and morphology etc. during humidifying–dehumidifying processes attract extensive attention, whereas the chemical reactions between coexisting components in mixed particles have been largely neglected. In a previous study, we found that substitution of a strong acid ( $HNO_3$ ) by a weaker acid ( $H_2C_2O_4$ ) takes place during vapor absorption in  $Ca(NO_3)_2/H_2C_2O_4$  mixtures because of the formation of less hygroscopic  $CaC_2O_4$  particles.<sup>51</sup> In the

present study, substitution of chloride by oxalate was also found. However, substitution of chloride by malonate and succinate hardly occurred during the humidifying and dehumidifying process of malonic acid–NaCl mixtures and succinic acid–NaCl mixtures. These results suggest that the hygroscopicity of a sodium dicarboxylate plays a critical role in the reaction between DCAs and NaCl during the humidifying and dehumidifying process. This possibility, that chemical reaction can occur, should be considered in future hygroscopic behavior studies of mixtures, although the present experiments were performed using bulk measurements and the results may sometimes differ from those obtained from individual particles.

Moreover, due to the important role of the Cl atom in atmospheric chemistry, much attention has been paid to the atmospheric processes which lead to the depletion of chloride in sea-salt particles in laboratory, field, and modeling studies.<sup>6</sup> Substitution of Cl in sea-salt particles by organic anions was suggested by Kerminen et al.<sup>19</sup> and Laskin et al.<sup>25</sup> Due to the high contribution of oxalic acid to the total mass of DCAs and organic aerosol, acid displacement reactions between oxalic acid and NaCl may play a significant role.

## ■ ASSOCIATED CONTENT

### 📄 Supporting Information

Additional information, including vapor sorption analyzer description, Raman spectra, and ATR-FTIR measurements. This material is available free of charge via the Internet at <http://pubs.acs.org>.

## ■ AUTHOR INFORMATION

### Corresponding Author

\*Phone: +86 10 62849123; fax: +86 10 62923563; e-mail: honghe@rcees.ac.cn.

### Notes

The authors declare no competing financial interest.

## ■ ACKNOWLEDGMENTS

This research was funded by National Natural Science Foundation of China (20937004 and 21107129) and the Strategic Priority Research Program of the Chinese Academy of Sciences (Grant No. XDB05010300).

## ■ REFERENCES

- (1) Orr, C., Jr.; Kurd, F.; Corbett, W. Aerosol size and relative humidity. *J. Colloid Sci.* **1965**, *13*, 472–482.
- (2) Charlson, R. J.; Schwartz, S. E.; Hales, J. M.; Cess, R. D.; Coakley, J. A.; Hansen, J. E.; Hofmann, D. J. Climate forcing by anthropogenic aerosols. *Science* **1992**, *255* (5043), 423–430.
- (3) Pilinis, C.; Pandis, S. N.; Seinfeld, J. H. Sensitivity of direct climate forcing by atmospheric aerosols to aerosol size and composition. *J. Geophys. Res.* **1995**, *100* (D9), 18,739–18,754.
- (4) Lewis, R.; Schwartz, E. *Sea Salt Aerosol Production: Mechanisms, Methods, Measurements and Models—A Critical Review*. American Geophysical Union: 2004; Vol. 152.
- (5) Rossi, M. J. Heterogeneous reactions on salts. *Chem. Rev.* **2003**, *103* (12), 4823–4882.
- (6) Finlayson-Pitts, B. The tropospheric chemistry of sea salt: A molecular-level view of the chemistry of NaCl and NaBr. *Chem. Rev.* **2003**, *103* (12), 4801–4822.
- (7) Dai, Q.; Hu, J.; Salmeron, M. Adsorption of water on NaCl (100) surfaces: Role of atomic steps. *J. Phys. Chem. B* **1997**, *101* (11), 1994–1998.
- (8) Xu, L.; Bluhm, H.; Salmeron, M. An AFM study of the tribological properties of NaCl (100) surfaces under moist air. *Surf. Sci.* **1998**, *407* (1), 251–255.
- (9) Cziczo, D.; Abbatt, J. Infrared observations of the response of NaCl, MgCl<sub>2</sub>, NH<sub>4</sub>HSO<sub>4</sub>, and NH<sub>4</sub>NO<sub>3</sub> aerosols to changes in relative humidity from 298 to 238 K. *J. Phys. Chem. A* **2000**, *104* (10), 2038–2047.
- (10) Foster, M.; Ewing, G. Adsorption of water on the NaCl (001) surface. II. An infrared study at ambient temperatures. *J. Chem. Phys.* **2000**, *112*, 6817–6826.
- (11) Hameri, K.; Laaksonen, A.; Vakeva, M.; Suni, T. Hygroscopic growth of ultrafine sodium chloride particles. *J. Geophys. Res.* **2001**, *106* (D18), 20,749–20,757.
- (12) Joutsensaari, J.; Vaattovaara, P.; Vestinen, M.; H. meri, K.; Laaksonen, A. A novel tandem differential mobility analyzer with organic vapor treatment of aerosol particles. *Atmos. Chem. Phys.* **2001**, *1* (1), 51–60.
- (13) Ebert, M.; Inerle-Hof, M.; Weinbruch, S. Environmental scanning electron microscopy as a new technique to determine the hygroscopic behaviour of individual aerosol particles. *Atmos. Environ.* **2002**, *36* (39–40), 5909–5916.
- (14) Krueger, B. J.; Grassian, V. H.; Iedema, M. J.; Cowin, J. P.; Laskin, A. Probing heterogeneous chemistry of individual atmospheric particles using scanning electron microscopy and energy-dispersive X-ray analysis. *Anal. Chem.* **2003**, *75* (19), 5170–5179.
- (15) Schuttlefield, J.; Al-Hosney, H.; Zachariah, A.; Grassian, V. H. Attenuated total reflection fourier transform infrared spectroscopy to investigate water uptake and phase transitions in atmospherically relevant particles. *Appl. Spectrosc.* **2007**, *61* (3), 283–292.
- (16) Ma, Q.; He, H.; Liu, Y. In situ DRIFTS study of hygroscopic behavior of mineral aerosol. *J. Environ. Sci.* **2010**, *22* (4), 555–560.
- (17) Ma, Q.; Liu, Y.; He, H. The utilization of physisorption analyzer for studying the hygroscopic properties of atmospheric relevant particles. *J. Phys. Chem. A* **2010**, *114*, 4232–4237.
- (18) Cohen, M.; Flagan, R.; Seinfeld, J. Studies of concentrated electrolyte solutions using the electrodynamic balance. 1. Water activities for single-electrolyte solutions. *J. Phys. Chem.* **1987**, *91* (17), 4563–4574.
- (19) Kerminen, V.-M.; Teinilä, K.; Hillamo, R.; Pakkanen, T. Substitution of chloride in sea-salt particles by inorganic and organic anions. *J. Aerosol Sci.* **1998**, *29* (8), 929–942.
- (20) Yao, X.; Fang, M.; Chan, C. K. Size distributions and formation of dicarboxylic acids in atmospheric particles. *Atmos. Environ.* **2002**, *36* (13), 2099–2107.
- (21) Johansen, A. M.; Siefert, R. L.; Hoffmann, M. R. Chemical characterization of ambient aerosol collected during the southwest monsoon and intermonsoon seasons over the Arabian Sea: Anions and cations. *J. Geophys. Res.* **1999**, *104* (26), 325–326.
- (22) Tervahattu, H.; Hartonen, K.; Kerminen, V.-M.; Kupiainen, K.; Aarnio, P.; Koskentalo, T.; Tuck, A. F.; Vaida, V. New evidence of an organic layer on marine aerosols. *J. Geophys. Res.* **2002**, *107* (D7), 4053.
- (23) Laskin, A.; Iedema, M. J.; Cowin, J. P. Quantitative time-resolved monitoring of nitrate formation in sea salt particles using a CCSEM/EDX single particle analysis. *Environ. Sci. Technol.* **2002**, *36* (23), 4948–4955.
- (24) Yao, X.; Fang, M.; Chan, C. K. Experimental study of the sampling artifact of chloride depletion from collected sea salt aerosols. *Environ. Sci. Technol.* **2001**, *35* (3), 600–605.
- (25) Laskin, A.; Moffet, R. C.; Gilles, M. K.; Fast, J. D.; Zaveri, R. A.; Wang, B.; Nigge, P.; Shutthanandan, J. Tropospheric chemistry of internally mixed sea salt and organic particles: Surprising reactivity of NaCl with weak organic acids. *J. Geophys. Res.* **2012**, *117*, D15302.
- (26) Chan, C. K.; Ha, Z.; Choi, M. Y. Study of water activities of aerosols of mixtures of sodium and magnesium salts. *Atmos. Environ.* **2000**, *34* (28), 4795–4803.
- (27) Kanakidou, M.; Seinfeld, J.; Pandis, S.; Barnes, I.; Dentener, F.; Facchini, M.; Van Dingenen, R.; Ervens, B.; Nenes, A.; Nielsen, C.

Organic aerosol and global climate modelling: A review. *Atmos. Chem. Phys.* **2005**, *5* (4), 1053–1123.

(28) Kawamura, K.; Ikushima, K. Seasonal changes in the distribution of dicarboxylic acids in the urban atmosphere. *Environ. Sci. Technol.* **1993**, *27* (10), 2227–2235.

(29) Chebbi, A.; Carlier, P. Carboxylic acids in the troposphere, occurrence, sources, and sinks: A review. *Atmos. Environ.* **1996**, *30* (24), 4233–4249.

(30) Mochida, M.; Kawabata, A.; Kawamura, K.; Hatsushika, H.; Yamazaki, K. Seasonal variation and origins of dicarboxylic acids in the marine atmosphere over the western North Pacific. *J. Geophys. Res.* **2003**, *108* (D6), 4193.

(31) Sullivan, R. C.; Prather, K. A. Investigations of the diurnal cycle and mixing state of oxalic acid in individual particles in Asian aerosol outflow. *Environ. Sci. Technol.* **2007**, *41* (23), 8062–8069.

(32) Wang, G.; Xie, M.; Hu, S.; Gao, S.; Tachibana, E.; Kawamura, K. Dicarboxylic acids, metals and isotopic compositions of C and N in atmospheric aerosols from inland China: Implications for dust and coal burning emission and secondary aerosol formation. *Atmos. Chem. Phys.* **2010**, *10*, 6087–6096.

(33) Rohrl, A.; Lammel, G. Low-molecular weight dicarboxylic acids and glyoxylic acid: Seasonal and air mass characteristics. *Environ. Sci. Technol.* **2001**, *35* (1), 95–101.

(34) Yang, L.; Yu, L. E. Measurements of oxalic acid, oxalates, malonic acid, and malonates in atmospheric particulates. *Environ. Sci. Technol.* **2008**, *42* (24), 9268–9275.

(35) Wang, G.; Kawamura, K.; Cheng, C.; Li, J.; Cao, J.; Zhang, R.; Zhang, T.; Liu, S.; Zhao, Z. Molecular distribution and stable carbon isotopic composition of dicarboxylic acids, ketocarboxylic acids, and  $\alpha$ -dicarbonyls in size-resolved atmospheric particles from Xi'an City, China. *Environ. Sci. Technol.* **2012**, *46* (9), 4783.

(36) Yu, J.; Huang, X.; Xu, J.; Hu, M. When aerosol sulfate goes up, so does oxalate: Implication for the formation mechanisms of oxalate. *Environ. Sci. Technol.* **2005**, *39* (1), 128–133.

(37) Sorooshian, A.; Lu, M. L.; Brechtel, F. J.; Jonsson, H.; Feingold, G.; Flagan, R. C.; Seinfeld, J. H. On the source of organic acid aerosol layers above clouds. *Environ. Sci. Technol.* **2007**, *41* (13), 4647–4654.

(38) Facchini, M.; Mircea, M.; Fuzzi, S.; Charlson, R. Cloud albedo enhancement by surface-active organic solutes in growing droplets. *Nature* **1999**, *401* (6750), 257–259.

(39) Yu, S. Role of organic acids (formic, acetic, pyruvic and oxalic) in the formation of cloud condensation nuclei (CCN): A review. *Atmos. Res.* **2000**, *53* (4), 185–217.

(40) Yang, F.; Chen, H.; Wang, X.; Yang, X.; Du, J.; Chen, J. Single particle mass spectrometry of oxalic acid in ambient aerosols in Shanghai: Mixing state and formation mechanism. *Atmos. Environ.* **2009**, *43* (25), 3876–3882.

(41) Peng, C.; Chan, M.; Chan, C. The hygroscopic properties of dicarboxylic and multifunctional acids: Measurements and UNIFAC predictions. *Environ. Sci. Technol.* **2001**, *35* (22), 4495–4501.

(42) Prenni, A.; DeMott, P.; Kreidenweis, S.; Sherman, D.; Russell, L.; Ming, Y. The effects of low molecular weight dicarboxylic acids on cloud formation. *J. Phys. Chem. A* **2001**, *105* (50), 11240–11248.

(43) Braban, C.; Carroll, M.; Styler, S.; Abbatt, J. Phase transitions of malonic and oxalic acid aerosols. *J. Phys. Chem. A* **2003**, *107* (34), 6594–6602.

(44) Wise, M. E.; Surratt, J. D.; Curtis, D. B.; Shilling, J. E.; Tolbert, M. A. Hygroscopic growth of ammonium sulfate/dicarboxylic acids. *J. Geophys. Res.* **2003**, *108* (20), 4638.

(45) Cruz, C. N.; Pandis, S. N. Deliquescence and hygroscopic growth of mixed inorganic-organic atmospheric aerosol. *Environ. Sci. Technol.* **2000**, *34* (20), 4313–4319.

(46) Francis, D.; Pope, B. J. D.-S.; Paul, T.; Griffiths; Simon, L.; Clegg; Cox, R. Anthony Studies of single aerosol particles containing malonic acid, glutaric acid, and their mixtures with sodium chloride. I. Hygroscopic growth. *J. Phys. Chem. A* **2010**, *114*, 5335–5341.

(47) Liu, Y. C.; Liu, C.; Ma, J. Z.; Ma, Q. X.; He, H. Structural and hygroscopic changes of soot during heterogeneous reaction with O<sub>3</sub>. *Phys. Chem. Chem. Phys.* **2010**, *12* (36), 10896–10903.

(48) Gysel, M.; Weingartner, E.; Baltensperger, U. Hygroscopicity of aerosol particles at low temperatures. 2. Theoretical and experimental hygroscopic properties of laboratory generated aerosols. *Environ. Sci. Technol.* **2002**, *36* (1), 63–68.

(49) Wise, M.; Biskos, G.; Martin, S.; Russell, L.; Buseck, P. Phase transitions of single salt particles studied using a transmission electron microscope with an environmental cell. *Aerosol Sci. Technol.* **2005**, *39* (9), 849–856.

(50) Ma, Q.; He, H.; Liu, C. Hygroscopic properties of oxalic acid and atmospherically relevant oxalates. *Atmos. Environ.* **2013**, *69*, 281–288.

(51) Ma, Q.; He, H. Synergistic effect in the humidifying process of atmospheric relevant calcium nitrate, calcite and oxalic acid mixtures. *Atmos. Environ.* **2012**, *50*, 97–102.

(52) Saxena, P.; Hildemann, L. Water absorption by organics: Survey of laboratory evidence and evaluation of UNIFAC for estimating water activity. *Environ. Sci. Technol.* **1997**, *31* (11), 3318–3324.

(53) Brooks, S.; Wise, M.; Cushing, M.; Tolbert, M. Deliquescence behavior of organic/ammonium sulfate aerosol. *Geophys. Res. Lett.* **2002**, *29* (19), 1917.

(54) Stokes, R.; Robinson, R. Interactions in aqueous nonelectrolyte solutions. I. Solute-solvent equilibria. *J. Phys. Chem.* **1966**, *70* (7), 2126–2131.

(55) Seinfeld, J.; Pandis, S., *Atmospheric Chemistry and Physics: From Air Pollution to Climate Change*; John Wiley: New York, 1998.

(56) Zdanovskii, A. New methods for calculating solubilities of electrolytes in multicomponent systems. *Zhur. Fiz. Kim* **1948**, *22*, 1475–1485.

(57) Peng, C.; Chan, C. K. The water cycles of water-soluble organic salts of atmospheric importance. *Atmos. Environ.* **2001**, *35* (7), 1183–1192.

(58) Wu, Z. J.; Nowak, A.; Poulain, L.; Herrmann, H.; Wiedensohler, A. Hygroscopic behavior of atmospherically relevant water-soluble carboxylic salts and their influence on the water uptake of ammonium sulfate. *Atmos. Chem. Phys.* **2011**, *11*, 12617–12626.

(59) Ebisuzaki, Y.; Angel, S. M. Raman study of hydrogen bonding in  $\alpha$  and  $\beta$ -oxalic acid dihydrate. *J. Raman Spectrosc.* **1981**, *11* (4), 306–311.

(60) Nieminen, J.; Rasanen, M.; Murto, J. Matrix isolation and ab initio studies of oxalic acid. *J. Phys. Chem.* **1992**, *96*, 5303–5308.

(61) Mohaček-Grošev, V.; Grdadolnik, J.; Stare, J.; Hadži, D. Identification of hydrogen bond modes in polarized Raman spectra of single crystals of  $\alpha$ -oxalic acid dihydrate. *J. Raman Spectrosc.* **2009**, *40* (11), 1605–1614.

(62) Frost, R. L. Raman spectroscopy of natural oxalates. *Anal. Chim. Acta* **2004**, *517*, 207–214.

(63) Haynes, W. M.; Lide, D. R. *CRC Handbook of Chemistry and Physics*; CRC Press: Boca Raton, FL, 2011

(64) Ma, Q.; Liu, Y.; Liu, C.; He, H. Heterogeneous reaction of acetic acid on MgO,  $\alpha$ -Al<sub>2</sub>O<sub>3</sub>, and CaCO<sub>3</sub> and the effect on the hygroscopic behaviour of these particles. *Phys. Chem. Chem. Phys.* **2012**, *14*, 8403–8409.

(65) Sullivan, R.; Moore, M.; Petters, M.; Kreidenweis, S.; Roberts, G.; Prather, K. Effect of chemical mixing state on the hygroscopicity and cloud nucleation properties of calcium mineral dust particles. *Atmos. Chem. Phys.* **2009**, *9*, 3303–3316.